4-2022

# Estimation of pure B power in polarized CMB data via Gibbs sampling.

Joseph Sterling
*University of Richmond*

# Estimation of pure B power in polarized CMB data via Gibbs sampling.

Joseph Sterling and Emory Bunn

*Physics Department, University of Richmond, Richmond, VA 23173, USA*

In the search for effective processes to estimate E and B spectra from polarized data, Gibbs Sampling has proven to be a powerful method. In the search for B modes, it is essential to avoid a false positive detection due to contamination from the larger E component. It is therefore of interest to combine Gibbs sampling with methods to "purify" the B modes, ensuring that a B-mode detection is robust. This goal can be achieved by compelling the Gibbs Sampler to estimate a pure B spectrum. The method we chose to implement involves an artificially inflated E spectrum, which "forces" the sampler to prefer to classify all ambiguous modes as E modes. If this method is to be useful, the resulting bias in the B spectrum must be small, and any increase in the error as compared to the "standard" sampler must be acceptable. We present Gibbs sampling analyses of simulated polarized sky data, in which we quantify these effects.

## I. INTRODUCTION

For the first 380,000 years after the Big Bang, the universe was opaque. Photons could not travel very far before encountering an electron and scattering. Once the universe cooled down to about 3000 K, the last scattering occurred, the result of which we can see as the CMB [1]. Due to the lack of interaction between CMB photons and matter after the last scattering, the CMB paints a canvas of the early universe. As such, it is a powerful tool that allows us to probe into fundamental elements of the cosmos [2].

When we scan the sky, we observe both the energy of the photons – an indicator of the temperature of the CMB – and polarization in the CMB [3] The intensity and polarization of the electro-magnetic spectrum radiating from the CMB can be broken down into the Stokes Parameters. Due to the conditions in the early universe at the moment of last scattering, the photons which make up the CMB was subjected to Thompson Scattering [3]. This induced

only linear polarization in the CMB which we observe as the Q and U components of the Stokes Parameters, with no V component – the temperature of the CMB represents the I component [3]. These observations result in 3 maps of the CMB: a T map, a Q map, and a U map. Each of the CMB maps can be represented by a list of values at each spherical coordinate on the sky and those lists in turn describe a function over the entire surface of the CMB sphere. This function can be represented by a combination of sin and cos functions, similar to a Fourier series. However, Fourier series specifically does not work on the surface of a sphere – breaking down near the poles. In order to properly analyze the function of the CMB maps using a linear combination of sin and cos, we must us a Spherical Harmonic expansion [3]. The amplitudes of the waves in the Spherical Harmonic Expansion are called the $a_{lm}$ coefficients and the entirety of the Spherical Harmonic Expansion can be represented by a list coefficients. The "$l$'s" are related to the frequency and the "$m$'s" describe the polarization in different directions. For each $l$, there are $(2l + 1)m$'s associated with it ($l = 2$ has $m = -2, -1, 0, 1, 2$, for example). The variance, or the mean-square, of each set of $l$'s and $m$'s is known as the power spectra of the map and is labled as $C_l$ A. Our current models of the universe suggest that the polarization which makes up the Q and U maps is made from two different power spectra: B-modes and E-modes [3].

## Inflation

The prevailing theory of how the early universe behaved is called inflation [2]. It solves problems in the standard model of physics by positing that the very beginning of the universe was followed by a rapid expansion [2]. One of the consequences of this is the prediction of fluctuation in the early universe, known as "scalar" and "tensor" type fluctuations [2]. The scalar fluctuations were the result of the mass density variations of the universe [2]. These resulted in only E-modes being created. The tensor fluctuations arose from quantum fluctuation (including gravitational waves) and created both E and B modes in roughly equal amounts [2]. The modes from each source combined, hence why E-modes are so much stronger than B-modes [2].

**Detection of B-modes**

As power spectra (T, E, and B) decrease as associated angular scale increases, finding B-Modes at large angular scales is quite difficult. In order to search for B-modes at large angular scales, future researchers will have to estimate the B-mode power spectra from their gathered data. However, this will be difficult due to the contamination of the E-mode's power [4] All observations of the CMB will contain both E and B modes. Since no method of separation is perfect, there will always be questions as to whether the strong E-modes are contaminating the weak B modes. There are ways to get around this impediment. One process is to answer the question probabilistically. "How probable is it that an observed map was made out of just E modes, versus the probability of having both?" The result of this line of questioning is a probability distribution, which can be explored via a process known as Gibbs Sampling [5] A probability curve near zero at a B power spectrum of zero implies that it is very unlikely that a CMB with no B-modes would produce the data that we observed.

## II. GIBBS SAMPLING

Gibbs Sampling is a Markov-Chain-Monte-Carlo (MCMC) algorithm based in Bayesian interpretation of probability used to obtain observations within a multivariate probability distribution. Gibbs Sampling is best utilized when sampling from the joint probability distribution $\left( p(x_1, x_2, \cdots) \right)$ is difficult but sampling from the conditional probability densities $\left( p(x_1|x_2, \cdots), p(x_2|x_1, \cdots), \cdots \right)$ is relatively easy, be it in the form of either computational complexity or computational time. This is true of our problem due to the lack of an exact one-to-one relationship between a CMB power spectrum and map and due to the mixing of the E mode and B mode power.

A Gibbs Sampler being used on a two-dimensional probability distribution can be broken down into 4 steps:

1) Begin with a "best guess" (or prior) within the joint probability distribution: $(x_0, y_0)$.

2) Generate a new $x$ sample by using the conditional probability of $x$ given $y_0$: $x_1 \sim p(x|y_0)$.
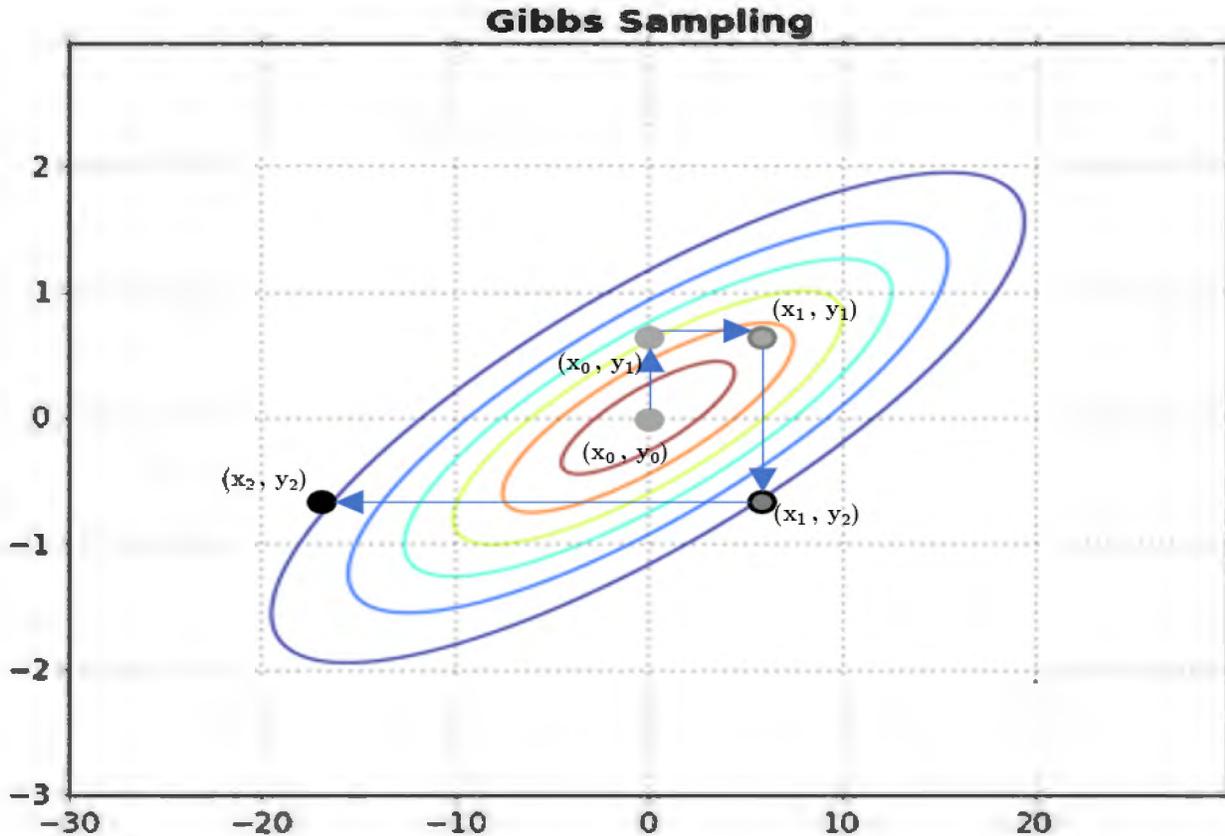
FIG. 1. The figure contains a joint Normal distribution with arbitrary $x$ and $y$. The points are example steps made by a Gibbs Sampler. The point at the center $(x_0, y_0)$, is the initial guess and the points $(x_1, y_1)$ and $(x_1, y_1)$ are the results of the first two runs of the the Gibbs Sampler. The arrows represent the movement resulting from each step of the Sampler.

3) Generate a new $y$ sample using the result of step 2 as the given: $y_1 \sim p(y|x_1)$.

4) Save the resulting probability sample (or posterior) and rerun the sampler with $(x_1, y_1)$ serving as the new prior.

By repeating this process for a long enough period of time, we are able to sample the entry of the joint-probability distribution, as seen in Figure 1.

## III.   METHODS

There is no one-to-one operation for moving between maps and power spectra. Each map can be produced by multiple power spectra, and each power spectra can generate multiple maps, with each process resulting in a probability distribution. Combining these two creates a multi-dimensional probability space of power spectra and CMB maps. Sampling from a

multi-dimensional probability space is very difficult; however, sampling from conditional probability distributions is much simpler. To leverage the relative simplicity of sampling from conditional probability distributions in order to sample the multi-dimensional spectra-map probability space, we will use Gibbs Sampling. For the Gibbs Sampler to work, we need an initial guess of the multi-dimensional spectra-map probability. This should take the form of an observed map of the CMB and probable power spectra. However, the actual data collected from a telescope is a map of the sky which contains both the actual CMB map – called the "signal" map – as well as some noise due to the telescope. As such, the Gibbs Sampler can be broken up into 4 steps:

1) Take in an observed map of the CMB (data) and an initial guess power spectra

2) Generate a possible signal map using the data and guess power spectra

3) Generate a guess power spectra using the generated map

4) Repeat from step 1 with the guess power spectra being the result from step 3

This process results in a list of power spectra, all of which could have resulted in the current CMB we see today with more power spectra being close to the actual power spectra. In order to run the Gibbs Sampler, we will be using the method outlined in Estimation of Polarized Spectra by Gibbs Sampling by Larson et. all. [6]

**Gibbs Sampler: Step 1**

To begin, we will identify the objects used in the mathematical operations for a one-map observation of the CMB. Maps of the CMB are broken up into pixels such that each pixel represents the same area of the sphere utilizing the HEALPix [1] method, with the total number referred to as *npix* [7][8].

The pixels of each map can be represented as a vector beginning at the "north" pole and circling around and around the sphere at each latitude level ending at the "south" pole (the actual orientation does not matter, as long as it is consistent over the entire process). The observed map is given a special label, $\vec{d}$. The noise in $\vec{d}$ can be approximated as a map of Gaussian fluctuations with some constant variance for every pixel, known as the noise
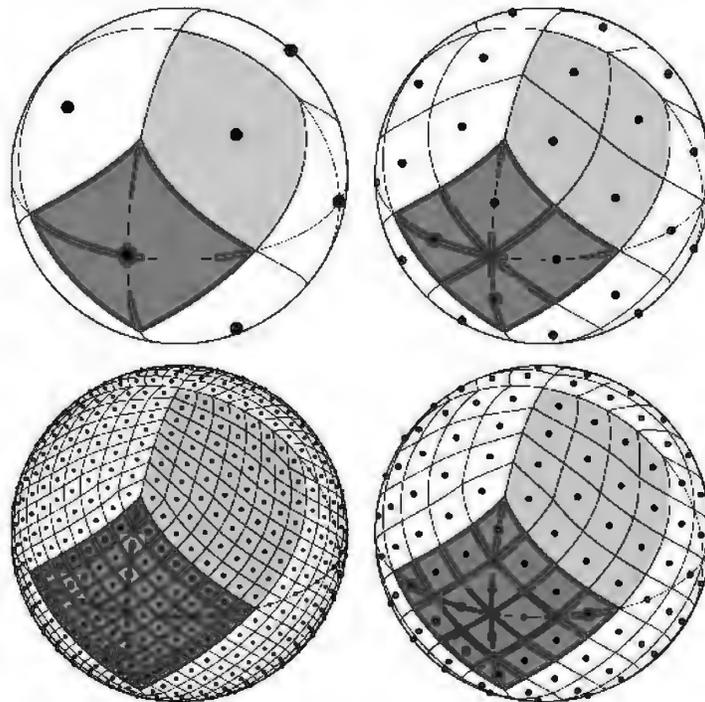
---

[1] http://healpix.sourceforge.net

FIG. 2. The top left figure shows the minimum number of pixels ($npix = 12$). Each pixel can further be divided into four new pixels. The number of pixels which fit on the edge of the original pixels is referred to as $nside$. This is done once in the top right figure, resulting in $npix = 48(nside = 2)$. This process is repeated once again in the bottom right figure ($npix = 192(nside = 4)$) and again in the bottom left ($npix = 768(nside = 8)$). [7][8]

covariance. The noise variance is represented in the Gibbs Sampler by the $npix \times npix$ diagonal matrix $N$. The guess power spectra is represented by the diagonal matrix $S$.

**Gibbs Sampler: Step 2**

Step 2 of the Gibbs Sampler can be represented as [6]:

$$s \sim P(\text{signal maps}|C_l, \vec{d}) \tag{1}$$

To generate the most probable sample map, we will use a process known as the Wiener Filter [9]. The Wiener Filter groups all of the $S, N$, and $\vec{[d]}$ associated with the three maps together to solve a large system of equations. It then utilizes the conjugate gradient method to solve for the most probable map. Without going into too much detail A, the conjugate gradient methods solves a matrix equation in the form of $Az_x = b_x$, where $A$ is a known

matrix or linear operator, $b_x$ is a known vector, while $z_x$ is an unknown vector. The actual equation takes the form of [6]:

$$\left(1 + S^{\frac{1}{2}}N^{-1}S^{\frac{1}{2}}\right)S^{-\frac{1}{2}}x = S^{\frac{1}{2}}N^{-1}\vec{d} \tag{2}$$

Where $\left(1 + S^{\frac{1}{2}}N^{-1}S^{\frac{1}{2}}\right) = A$, and $S^{-\frac{1}{2}}x = z_x$ and $S^{\frac{1}{2}}N^{-1}\vec{d} = b_x$. $S^{-\frac{1}{2}}x$ is then multiplied by $S^{\frac{1}{2}}$ to produce $x$, the most probable map.

However, the Wiener filter only reconstructs the parts of the signal map that are well-determined from the data [9]. This leads to two important behaviors:

1. The Wiener filter is an incredibly consistent process – it is not suitable as a method to sample from a conditional probability on its own.

2. Over time, the Wiener filter will cut down the range of values of the sample maps. This results in sample maps with small data points, which would correspond to a Universe with no CMB – one we certainly do not live in.

To reintroduce the parts of the signal that are not well defined (and maintain that our sample maps show the existance of the CMB), we will add back in some randomness to generate a probable map with the entire range of values [6]. This is done in a similar way to the Weiner filter, as seen in the equation below [6].

$$\left(1 + S^{\frac{1}{2}}N^{-1}S^{\frac{1}{2}}\right)S^{-\frac{1}{2}}y = \xi + S^{\frac{1}{2}}N^{-\frac{1}{2}}\chi \tag{3}$$

Where $S$ and $N$ are the same, but $\xi$ and $\chi$ are normal variates (also referred to as independent Gaussian random variates) [6]. Again, $S^{-\frac{1}{2}}y$ is then multiplied by $S^{\frac{1}{2}}$ to produce $y$, a random fluctuation map. By adding the Weiner filter map $x$ with the fluctuation map $y$, we arrive the true sample map [6].

$$s = x + y \tag{4}$$

**Gibbs Sampler: Step 3**

Step 3 of the Gibbs Sampler can be represented as [6]:

$$C_l \sim P(\text{power spectra}|s) \tag{5}$$

To complete Step 3, we will utilize the $a_{lm}$ coefficients of the sample map $s$. For each $l$, we compute $\sigma_l = \sum_{m=-l}^{+l} |s_{lm}^i|^2$ [6]. Afterwards, we generate a $(2l - 1)$ vector $p_l$ of Gaussian random variates with zero mean and unit variance [6]. From there, we calculate a possible $C_l$ for the sample map using the equation below [6].

$$C_l = \frac{\sigma_l}{|p_l|^2}, \text{ Where } |p_l|^2 \text{is the square norm of } p_l \tag{6}$$

**Gibbs Sampler: Step 4**

From here, we save the result of step 3 and update the guess power spectra to be the result of step 3 and feed it back into the Gibbs Sampler [6]. With enough iterations, we will sample from the entire map-power spectra probability distribution [5]. By employing statistical analysis techniques, we analyze the resulting list of probable power spectra to identify aspects of the probability distribution of power spectra.

## IV. TESTING

In order to test the Gibbs Sampler, we must know both the true power spectra of the CMB and a scan of the entire CMB. These are not known to us (otherwise this would be a redundant paper), so we must craft a method to generate a scan of the CMB with known power spectra. To do this, we utilized the NASA Goddard Space Flight Center website, `https://lambda.gsfc.nasa.gov/toolbox/tb_camb_form.cfm`, to obtain a "true" $T$, $E$, and $B$ power spectra [10]. The website generates power spectra from earlier observations [10].

From there we utilized the Healpy python package to generate maps from the power spectra; this is labeled as our "true" maps. However, the Gibbs Sampler is supposed to require scans from a telescope, so we must add noise to our "true" maps to approximate a

data set. To do this, we generated random-normal fluctuation maps with a variance based on some fraction of the standard deviation of the "true" maps such that $\sigma^2_{noise} = \frac{\sigma_{true}}{noise\_frac}$. Then, we added them to the "true" maps, thus creating a data map, or $\vec{d}$. The variance of each noise map was saved as the matrix $N$ and the "true" spectra created the matrix $S$. We then passed all of these values into the Gibbs Sampler and compared the resulting list of generated power spectra to the "true" power spectra for $T$, $E$, and $B$ modes.

## V. RESULTS

When running tests on the Gibbs Sampler, we wished to investigate how it dealt with different amounts of noise in the data. To do this, we simply changed $noise\_frac$ to different values while keeping everything else the same. The tests were run with $n\_side = 16$ 2 and the Gibbs Sampler running for 1000 iterations. During our tests, an unexpected behavior emerged between $noise\_frac = 1000$ ( 3) and $noise\_frac = 10000$ ( 4).
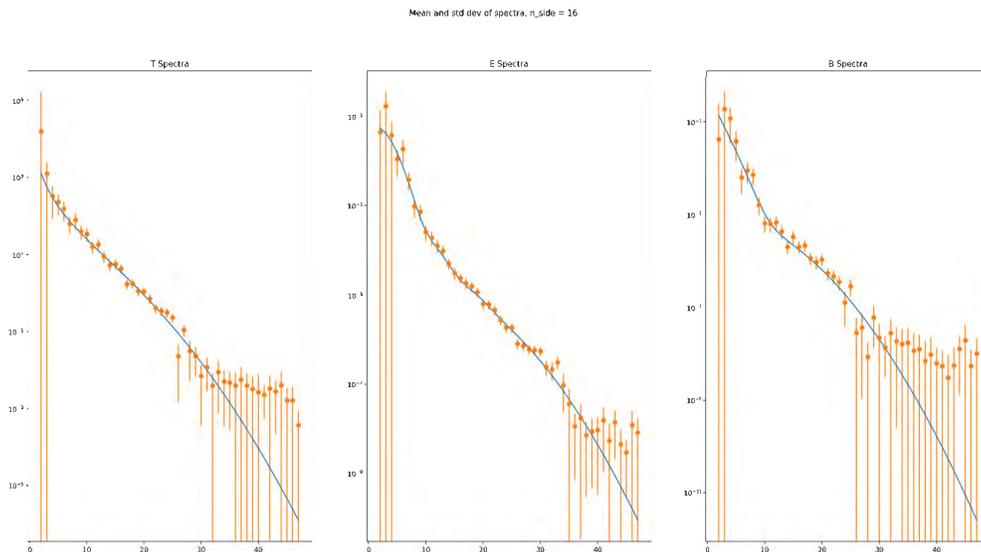


FIG. 3. Graphs the "true" power spectrum (blue line) against the mean and standard deviation of the results of the Gibbs Sampler (orange points with lines). The T spectrum is the leftmost, the E spectrum is the middle one, and the B spectrum is the rightmost. All of them are plotted with a logarithmic scale on the y-axis. This sampler was run with $noise\_frac = 1000$.

In Figure 3, the Gibbs Sampler appears to be functioning as intended. The "true" power spectrum falls within 2 standard deviations of the mean of the generates samples for each $l$. The slight over-estimation of the T, E, and B-modes can be accounted for by a
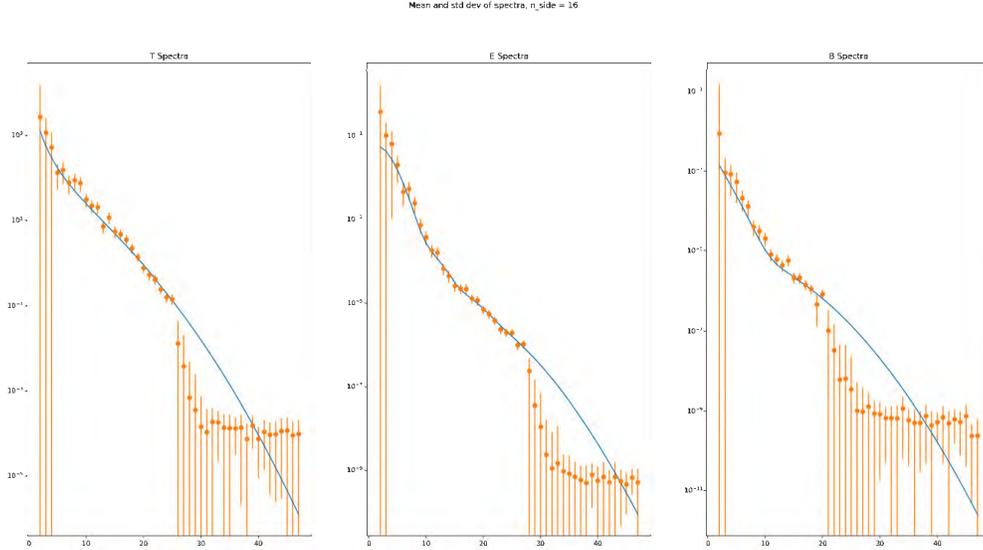
FIG. 4. Graphs the "true" power spectrum (blue line) against the mean and standard deviation of the results of the Gibbs Sampler (orange points with lines). The T spectrum is the leftmost, the E spectrum is the middle one, and the B spectrum is the rightmost. All of them are plotted with a logarithmic scale on the y-axis. This sampler was run with $noise\_frac = 10000$

phenomenon known as Cosmic Variance [2]. However, when $noise_f rac$ is increased to 10000 (thus reducing the variance of the noise), an unanticipated result occurs, as seen in Figure 4. For low to mid $l$, the generated power spectra follow the expected value nicely. But, at around $l = 26$ in the T spectra, $l = 28$ in the E spectra, and $l = 21$ in the B spectra, a noticeable drop occurs the values of the generated spectra until high $l$'s (around $l \geq 40$). Via inspection, we notice that the gen drop appears to separate the generated power spectra into two disjointed groups, one before the drop which behaves as expected, and one after the drop which does not. This type of behavior is not easily explained by Cosmic Variance [2].

## $l$ by $l$ investigation

To further inspect this unforeseen behavior, we examined the values of the generated T spectrum for specific $l$'s over all iterations of the Gibbs Sampler and compared them to the "true" power spectrum. Here we will look at that value over iterations for $l = 25$ (Figure 5) (before the drop) and $l = 26$ (Figure 6) and $l = 27$ (Figure 7) (both after the drop) for
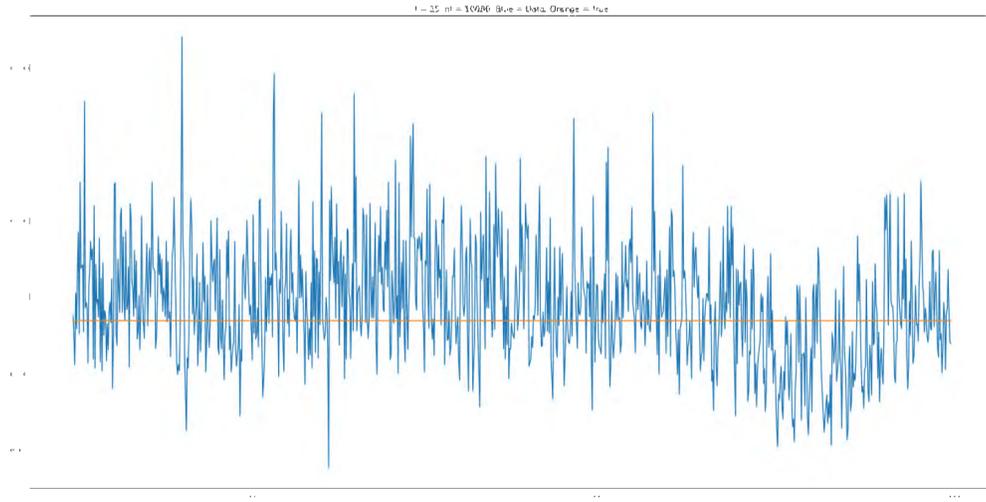
FIG. 5. A graph of the value of $l = 25$ for each of the 1000 Gibbs Sampler iterations for the T spectrum with $noise\_frac = 10000$. The blue line is the value of the generated spectrum at $l = 25$. The orange line is the value of the "true" T spectrum at $l = 25$.
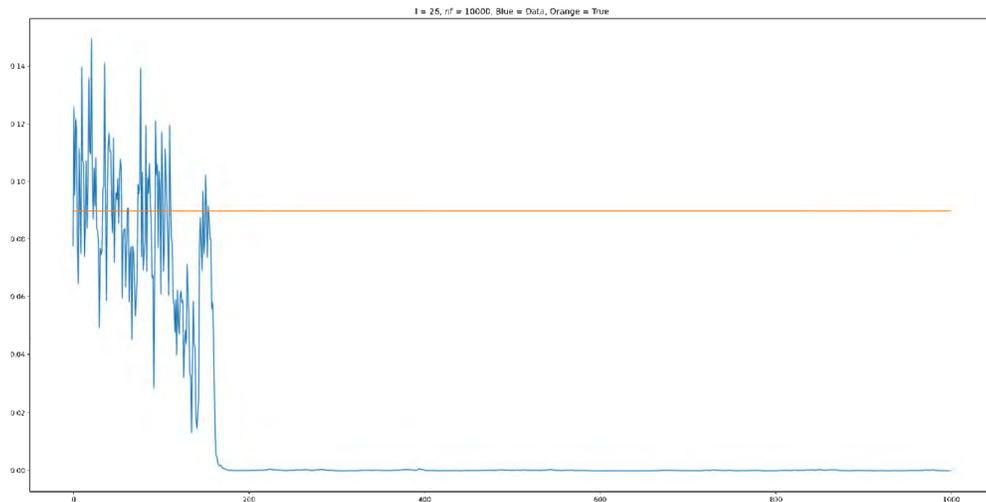
the T spectrum.



FIG. 6. A graph of the value of $l = 26$ for each of the 1000 Gibbs Sampler iterations for the T spectrum with $noise\_frac = 10000$. The blue line is the value of the generated spectrum at $l = 26$. The orange line is the value of the "true" T spectrum at $l = 26$.

As seen in Figure 5, for $l$'s that behave normally in the Gibbs Sampler, the value at each
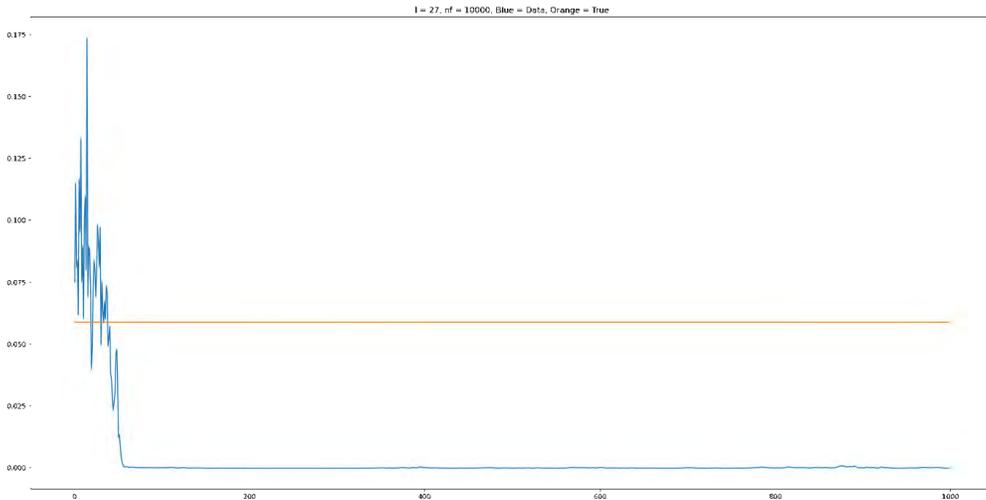
FIG. 7. A graph of the value of $l = 27$ for each of the 1000 Gibbs Sampler iterations for the T spectrum with $noise\_frac = 10000$. The blue line is the value of the generated spectrum at $l = 27$. The orange line is the value of the "true" T spectrum at $l = 27$.

iteration fluctuates round the "true" value. However, for the $l$'s after the drop, the behavior is not as well behaved. While the values in Figure 6 and Figure 7 begin at the appropriate level, they quickly fall off to near 0. This happens around the $180^{th}$ iteration in Figure 6, while happening even earlier – around the $60^{th}$ iteration – in Figure 7. This happens because the Gibbs Sampler is estimates a low value for those $l$ during a certain iteration, but for some reason continues to estimate them as low. The exact reasoning behind this unexpected behavior must by identified, understood, and corrected before further research may continue.

## VI. CONCLUSION

While the detection of B-modes remains elusive for now, we remain optimistic that Gibbs Sampling will yield interesting results a tool for sampling the multi-dimensional probability space of power spectra and CMB signal maps. We have tested the sample signal map generator and are confident is is preforming as intended. Our next point of examination is the sample power spectra generator. We believe that this is where the anomalous behavior originates. At some iteration, the sample power spectra generator section of the Gibbs

Sampler uses a signal map and returns a sample power spectra which is not large enough. Due to the iterative nature of the Gibbs Sampler, this "small" spectra is fed back in as the guess power spectra, which results in a signal map that is not a probable map of the "true" CMB. This process repeats until the Gibbs Sampler returns 0's (or numbers very close to 0) as guesses for the power spectra at certain $l$'s.

Once the Gibbs Sampler has been corrected and is performing as intended, we will be able to move onto pure B-Mode Sampling.

## Pure B Modes

As mentioned in the introduction, the fundamental problem with detecting B modes is the mixing with the much more powerful E modes. As seen above, Gibbs Sampling can be a powerful tool in alleviating this predicament, but our method comes with a structural flaw: the existence of modes is determined probabilistically. Due to the probabilistic mechanism the Gibbs Sampler uses to differentiate the E and B modes in the sample power spectra, it may return results that indicate the existence of B modes, even if they do not exist (and thus our models of the cosmos are flawed). To fix this possible discrepancy between our results and reality, we implement a minor change to the testing process which modifies our method to create a "pure B mode" Gibbs Sampler [4] [9]. By overestimating the magnitude of the E modes in our power spectra guess each iteration, we compel the Gibbs Sampler to assign all of the questionable modes as E modes [4] [9]. This means that any modes left over *must* be B modes. By applying the same statistical analysis to the resulting "Pure B" sample power spectra, we are able to determine how likely it is that B modes exist at all with a 95% probability [4] [9]. Since our Pure B mode Gibbs Sampler absorbed all of the uncertain modes into the E modes, it is highly likely that that actual magnitude of the B-modes is higher. Thus, we will lend even more credence to our current understand of the universe and inflation.

## Future Research

After properly implementing Pure B-mode sampling, there are several ways this research may proceed forward. These include simply running the pure B-mode Gibbs Sampler with

a higher *nside* and for more iterations, thus sampling for even larger $l$'s in the power spectra with higher accuracy. A different path forward would be to implement partial sky data. This would be a way to simulate that data received from a telescope does not cover the entire sky, leaving sections of the data to assume enough noise to completely drown out the signal for those pixels. In fact, the Wiener filter is an incredibly powerful tool for analysis partial sky data as it can utilise the exiting data to guess probable values for the missing pixels [9]. Another possible path would be to modify the Gibbs Sampler to handle some correlation between the T-spectrum and the E-spectrum [11]. The need to detect B-modes will continue to provide avenues for research for years to come.

## VII. ACKNOWLEDGEMENTS

[1] Barbara Ryden. *Introduction to Cosmology*. Cambridge University Press, 2 edition, 2002.

[2] Scott Dodelson. *Modern Cosmology*. Academic Press, 2003.

[3] Matias Zaldarriaga and Uroš Seljak. All-sky analysis of polarization in the microwave background. *Phys. Rev. D*, 55(4):1830–1840, February 1997.

[4] Emory F. Bunn, Matias Zaldarriaga, Max Tegmark, and Angelica de Oliveira-Costa. E/B decomposition of finite pixelized CMB maps. *Phys. Rev. D*, 67(2):023501, January 2003.

[5] Benjamin D. Wandelt, David L. Larson, and Arun Lakshminarayanan. Global, exact cosmic microwave background data analysis using Gibbs sampling. *Phys. Rev. D*, 70(8):083511, October 2004.

[6] Benjamin D. Wandelt, David L. Larson, and Arun Lakshminarayanan. Global, exact cosmic microwave background data analysis using Gibbs sampling. *Phys. Rev. D*, 70(8):083511, October 2004.

[7] Andrea Zonca, Leo Singer, Daniel Lenz, Martin Reinecke, Cyrille Rosset, Eric Hivon, and Krzysztof Gorski. healpy: equal area pixelization and spherical harmonics transforms for data on the sphere in python. *Journal of Open Source Software*, 4(35):1298, March 2019.

[8] K. M. Górski, E. Hivon, A. J. Banday, B. D. Wandelt, F. K. Hansen, M. Reinecke, and M. Bartelmann. HEALPix: A Framework for High-Resolution Discretization and Fast Analysis of Data Distributed on the Sphere. *Astrophys. J.*, 622:759–771, April 2005.

[9] Emory F. Bunn and Benjamin Wandelt. Pure E and B polarization maps via Wiener filtering. *Phys. Rev. D*, 96(4):043523, August 2017.

[10] Planck Collaboration, N. Aghanim, Y. Akrami, M. Ashdown, J. Aumont, C. Baccigalupi, M. Ballardini, A. J. Banday, R. B. Barreiro, N. Bartolo, S. Basak, R. Battye, K. Benabed, J. P. Bernard, M. Bersanelli, P. Bielewicz, J. J. Bock, J. R. Bond, J. Borrill, F. R. Bouchet, F. Boulanger, M. Bucher, C. Burigana, R. C. Butler, E. Calabrese, J. F. Cardoso, J. Carron, A. Challinor, H. C. Chiang, J. Chluba, L. P. L. Colombo, C. Combet, D. Contreras, B. P. Crill, F. Cuttaia, P. de Bernardis, G. de Zotti, J. Delabrouille, J. M. Delouis, E. Di Valentino, J. M. Diego, O. Doré, M. Douspis, A. Ducout, X. Dupac, S. Dusini, G. Efstathiou, F. Elsner, T. A. Enßlin, H. K. Eriksen, Y. Fantaye, M. Farhang, J. Fergusson, R. Fernandez-Cobos, F. Finelli, F. Forastieri, M. Frailis, A. A. Fraisse, E. Franceschi, A. Frolov, S. Galeotta, S. Galli, K. Ganga, R. T. Génova-Santos, M. Gerbino, T. Ghosh, J. González-Nuevo, K. M. Górski, S. Gratton, A. Gruppuso, J. E. Gudmundsson, J. Hamann, W. Handley, F. K. Hansen, D. Herranz, S. R. Hildebrandt, E. Hivon, Z. Huang, A. H. Jaffe, W. C. Jones, A. Karakci, E. Keihänen, R. Keskitalo, K. Kiiveri, J. Kim, T. S. Kisner, L. Knox, N. Krachmalnicoff, M. Kunz, H. Kurki-Suonio, G. Lagache, J. M. Lamarre, A. Lasenby, M. Lattanzi, C. R. Lawrence, M. Le Jeune, P. Lemos, J. Lesgourgues, F. Levrier, A. Lewis, M. Liguori, P. B. Lilje, M. Lilley, V. Lindholm, M. López-Caniego, P. M. Lubin, Y. Z. Ma, J. F. Macías-Pérez, G. Maggio, D. Maino, N. Mandolesi, A. Mangilli, A. Marcos-Caballero, M. Maris, P. G. Martin, M. Martinelli, E. Martínez-González, S. Matarrese, N. Mauri, J. D. McEwen, P. R. Meinhold, A. Melchiorri, A. Mennella, M. Migliaccio, M. Millea, S. Mitra, M. A. Miville-Deschênes, D. Molinari, L. Montier, G. Morgante, A. Moss, P. Natoli, H. U. Nørgaard-Nielsen, L. Pagano, D. Paoletti, B. Partridge, G. Patanchon, H. V. Peiris, F. Perrotta, V. Pettorino, F. Piacentini, L. Polastri, G. Polenta, J. L. Puget, J. P. Rachen, M. Reinecke, M. Remazeilles, A. Renzi, G. Rocha, C. Rosset, G. Roudier, J. A. Rubiño-Martín, B. Ruiz-Granados, L. Salvati, M. Sandri, M. Savelainen, D. Scott, E. P. S. Shellard, C. Sirignano, G. Sirri, L. D. Spencer, R. Sunyaev, A. S. Suur-Uski, J. A. Tauber, D. Tavagnacco, M. Tenti, L. Toffolatti, M. Tomasi, T. Trombetti, L. Valenziano, J. Valiviita, B. Van Tent, L. Vibert, P. Vielva,

F. Villa, N. Vittorio, B. D. Wandelt, I. K. Wehus, M. White, S. D. M. White, A. Zacchei, and A. Zonca. Planck 2018 results. VI. Cosmological parameters. *Astron. Astrophys.*, 641:A6, September 2020.

[11] D. L. Larson, H. K. Eriksen, B. D. Wandelt, K. M. Górski, Greg Huey, J. B. Jewell, and I. J. O'Dwyer. Estimation of Polarized Power Spectra by Gibbs Sampling. *Astrophys. J.*, 656(2):653–660, February 2007.

[12] William H. Press. *Numerical Recipes: The Art of Scientific Computing.* Cambridge University Press, 2007.

## Appendix A: Conjugate Gradient

The conjugate gradient method is a algorithm for solving a system of equations [12]. While the specifics of the technique are outside the scope of this paper, we would be remissed if we did not include something about it, especially considering how heavily we rely on it to generate our sample signal maps. Consider the following analogy:

Imagine there exists some parabola. The actual equation is unknown, but given a particular $x$-value, the corresponding value on the parabola can be found, along with it's derivative. You are trying to find the $x$-value at the minimum of the parabola (where the derivative equals 0). The conjugate gradient algorithm is such (Figure 8) :

1. Guess an $x$-value and find it's corresponding point on the parabola

2. Find the derivative at that point.

3. According to the sign and value of the derivative, take a step of a certain size (larger derivative, larger step)

4. use this new $x$-value as a new guess

5. Repeat for $n$ times until the derivative of your guess point is 0 (Figure 9).

Now, it is almost impossible to randomly walk to the exact point where the derivative of the parabola is 0, so the conjugate gradient method allows for some error in the derivative. If the derivative is "close enough" to 0, then the guess $x$ is returned as the solution [12].
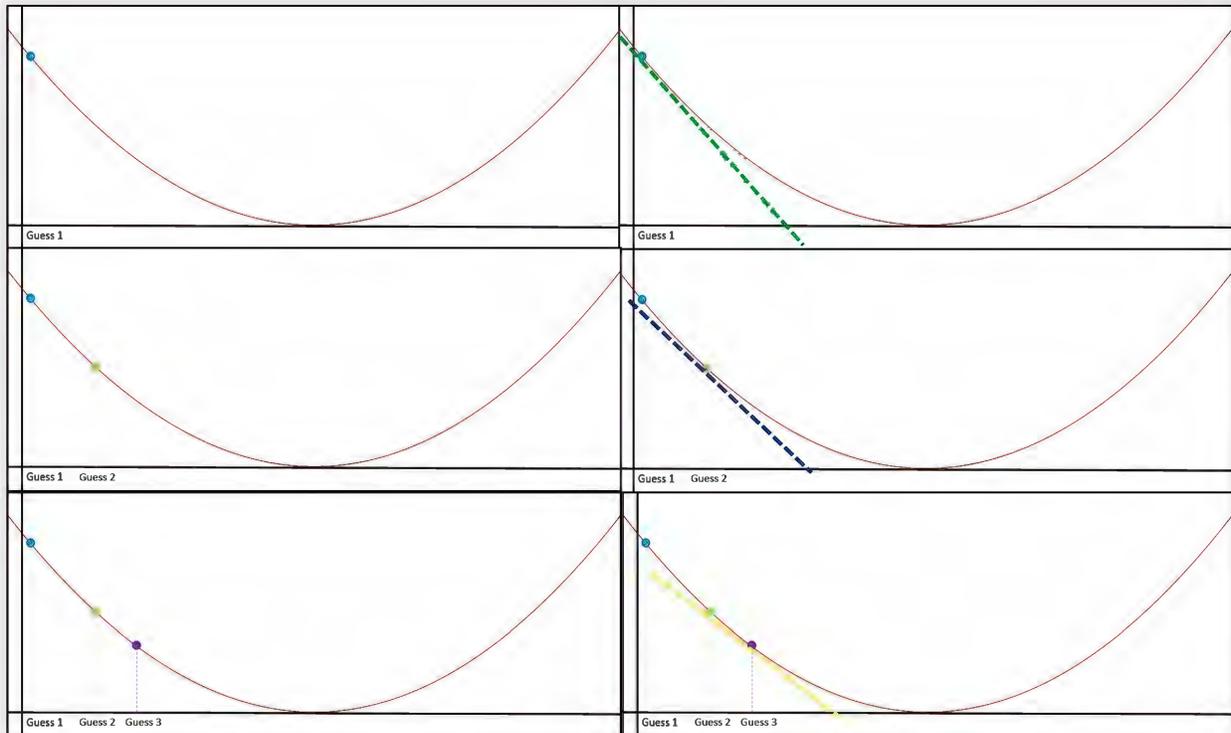
FIG. 8. **Top Left:** initial guess.
**Top Right:** derivative of the parabola at the point
**Middle Left:** Second guess
**Middle Right:** derivative of the parabola at the point
**Bottom Left:** Third guess. Notice that guess 2's derivative was less than guess 1's, so guess 3 is closer to guess 2 than guess 2 is to guess 1.
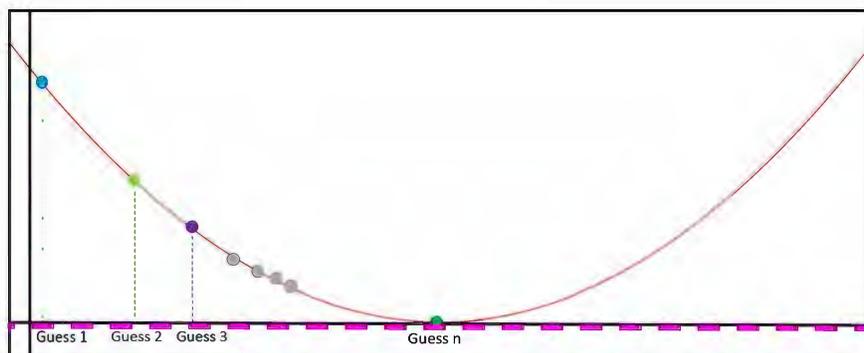**Bottom Right:** derivative of the parabola at the point



FIG. 9. The blue, lime, and purple dots are guesses 1, 2, and 3 from Figure 8. The grey dots are example guesses which were made in between guess 3 and guess $n$ (not every skipped guess is included). The green dot, guess $n$, is the final guess as it's associated derivative (in pink) is close enough to zero.

## Appendix A: power spectra exceptions

There are two notable neglections for the sower spectra: $l = 0$, and $l = 1$. As the $l$'s in the $a_{lm}$ coefficients and the power spectra $(C_l)$ are representative the number of peaks of the waves on the sphere, these correspond to the waves with 0 and 1 peak respectively.

For $l = 0$, that just corresponds to the average of the map [2]. For instance, the $l = 0$ term in the T-spectra corresponds to a map where each pixel is at $2.725 \ K$ with no variance [2]. This corresponds to the average temperature of the CMB. This result is not interesting and already well known, which combined with the strangeness that $l = 0$ can cause during calculations means that the $l = 0$ terms are not analysed.

For $l = 1$, it is excluded due to the Doppler effect [2]. Since $l = 1$ corresponds to wave with one peak, it's map would have a hot side and a cold side [2]. This phenomenon is observed, however, due to the earth's movement in the universe, it is impossible to tell if the difference in frequency of the CMB photons is actually caused by one side of the early universe having more energy, or by the Doppler shift of us moving toward on side [2]. Since it is impossible to accurately measure the $l = 1$ term, it is dropped from the analysis [2].